Materials Research Proceedings **20** (2022) 39-46 https://doi.org/10.21741/9781644901731-6

Consistent Modal Calibration of a Pendulum-Type Vibration Absorber

Jan Høgsberg

Department of Mechanical Engineering, Technical University of Denmark, Nils Koppels Alle, building 404, DK 2800 Kongens Lyngby, Denmark

jhg@mek.dtu.dk

Keywords: Vibration Absorber, Structural Dynamics, Modal Analysis, Absorber Calibration

Abstract. Pendulum absorbers are installation in offshore wind turbines to mitigate excessive vibration amplitudes from wind and wave loading. The pendulum damper is placed inside the tower and attached to the structure at two distinct points: The tower top, where the pendulum arm is fixated, and at the position of the pendulum mass, which is connected to the tower wall by the damper. The present paper derives a modal calibration principle, which consistently accounts for different points of attachment for the absorber stiffness and damping.

Introduction

Offshore wind turbines are among the most popular and effective renewable energy sources available today. In local areas with large water depth, such as in Norway, the classic foundation types are infeasible and thus floating platforms seem to be the most viable alternative. Absorber devices, such as a pendulum-type vibration absorber, may therefore be installed to compensate for the increased flexibility. The damping of offshore wind turbines is considered in greater detail in references [1-4].

Vibration absorbers are calibrated with respect to a single targeted vibration mode, with a well-defined natural frequency and mode shape [1, 5-7]. A modal system reduction then results in a two-degree-of-freedom (2-dof) model with a single mode coupled with the single-mass absorber. For the pendulum absorber the apparent stiffness connects the absorber mass to the tower-top, while the dashpot transfers the absorber force to the tower wall. This non-collocation implies a modelling error in the modal reduction, that may be taken into account be redefining the 'undamped' structure as the compound system with the absorber dashpot fully locked. When using the mode shape for this augmented undamped structural model, the scalar structural equation becomes less sensitive to any feedback from other vibration modes [8]. Furthermore, it retains the dynamic model associated with vanishing absorber damping as a case that can be used to calibrate for residual mode correction coefficients, which include the modal interaction with other vibration modes [9]. This correction is however not considered in the present analysis, which simply truncates any modal series representation to its single dominant term. The proposed calibration formulae in the present paper can be used in practice to improve the performance of pendulum dampers, as well as more advanced absorbers with flexible appendages.

The structural model

Assume a build-up FE model of the offshore wind turbine (owt) structure in Fig.1(a), with the pendulum-type vibration absorber attached inside the tower. When the pendulum behavior is linearized, the equation of motion can be written as

$$\mathbf{M}\ddot{\mathbf{q}} + \mathbf{C}\dot{\mathbf{q}} + \mathbf{K}\mathbf{q} = \mathbf{f} \tag{1}$$

with **M**, **C** and **K** representing the model mass matrix, damping matrix and stiffness matrix, respectively, while the vector **q** contains the general dofs of the combined structure-absorber dynamic model.

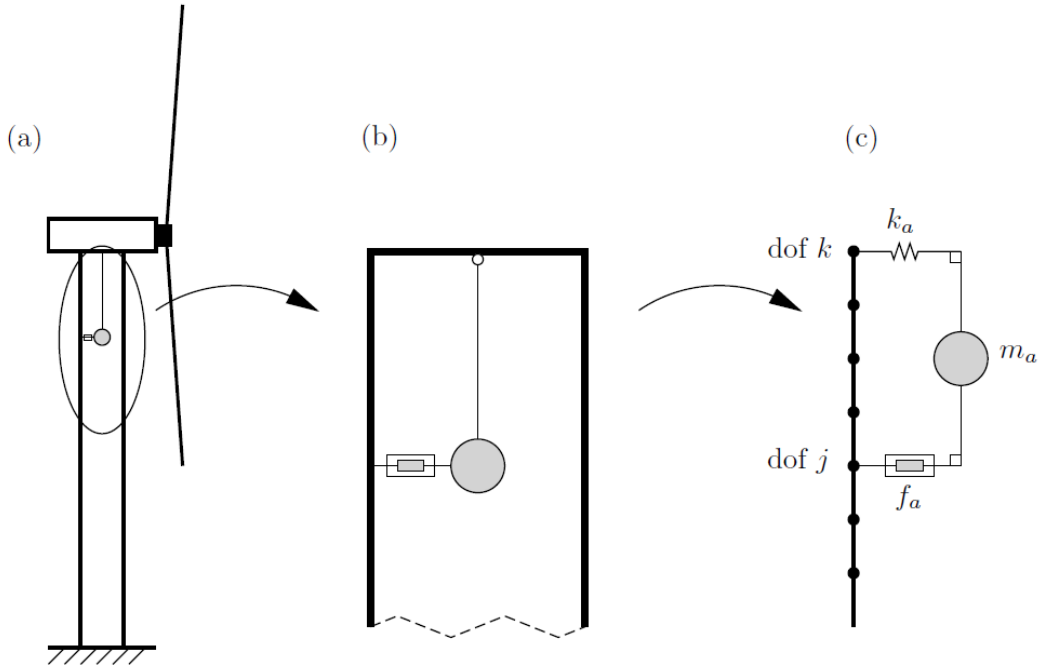

Figure 1: (a) Wind turbine with tower pendulum absorber, (b) close-up of pendulum with damper and (c) equivalent linearized model with damper force f_a at dof j and apparent spring from pendulum arm at an upper dof k.

The system is split by dividing the dofs into those associated with the structure and the supplemental dofs representing the absorber. It should be noted that common dofs are included in the structure. Hereby, the displacement vector can be decomposed as

$$\mathbf{q} = \begin{bmatrix} \mathbf{u}_s \\ u_a \end{bmatrix} \tag{2}$$

whereby the system matrices are correspondingly split as follows,

$$\mathbf{M} = \begin{bmatrix} \mathbf{M}_s & \mathbf{0} \\ \mathbf{0}^T & m_a \end{bmatrix} \quad , \quad \mathbf{C} = \begin{bmatrix} c_a\mathbf{d}\mathbf{d}^T & -c_a\mathbf{d} \\ -c_a\mathbf{d}^T & c_a \end{bmatrix} \quad , \quad \mathbf{K} = \begin{bmatrix} \mathbf{K}_s + k_a\mathbf{b}\mathbf{b}^T & -k_a\mathbf{b} \\ -k_a\mathbf{b}^T & k_a \end{bmatrix} \tag{3}$$

with subscripts *s* and *a* referring to *structure* and *absorber*, respectively. The non-identical connectivity vectors **b** and **d** are zero vectors with a single unit value at dof *k* and *j*, respectively.

Classic tuning method

The common tuning principle for vibration absorbers follows from the analysis of the so-called tuned mass damper (TMD) [5, 6], which corresponds to the pendulum damper in Fig. 1(c) with *j*=*k*. The dynamics of the structure are represented by the vibration mode $\bar{\mathbf{u}}_0$ governed by

Materials Research Proceedings **20** (2022) 39-46 https://doi.org/10.21741/9781644901731-6

$$\left(\mathbf{K}_s - \omega_0^2 \mathbf{K}_s\right)\bar{\mathbf{u}}_0 = \mathbf{0} \tag{4}$$

where ω_0 is the corresponding natural frequency of the virgin host structure. The calibration formulae for the classic TMD are

$$\kappa_0 = \frac{\mu_0}{(1+\mu_0)^2} \quad , \quad \beta_0 = \sqrt{2\mu_0^3(1-\mu_0)} \tag{5}$$

in which the modal mass ratio $\mu_0 = m_a/m_0$ determines the absorber mass m_a relative to the modal mass m_0 , the corresponding modal stiffness ratio $\kappa_0 = k_a/k_0$ defines the absorber stiffness k_a relative to the modal stiffness k_0, while the damper ratio $\beta_0 = c_a/\sqrt{k_0 m_0}$ represents the absorber viscous coefficient relative to the geometric mean of the modal mass and stiffness.

The modal mass m_0 and stiffness k_0 are not uniquely defined, as the absorber mass is attached at either dof j or k via the dashpot or spring, respectively. Figure 2 shows the frequency response curves for the top tower deflection u_{top} in (a) and the absolute absorber motion u_a in (b). The mode shape is normalized to unity at the top dof k for the red curve in Fig. 2, while the magenta curve represents the TMD tuning when the mode shape is normalized relative to the lower dof j, at which the absorber damper is connected.

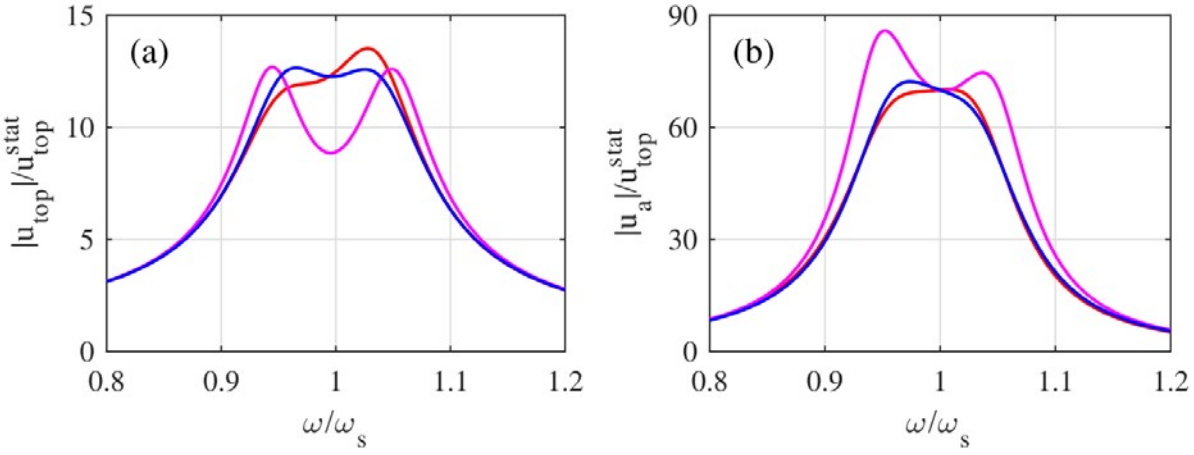

Figure 2: (a) Frequency amplitude curve for top tower motion (a) and for pendulum mass deflection (b).

Since the absorber mass m_a is constant, the modal mass ratio is $\mu_0 = 0.0154$ (red curve) for a top tower attachment at dof k, while at dof j it reduces to almost half $\mu_0 = 0.008$ (magenta curve) because of the reduced deflection at the lower position. It is seen from Fig. 2 that the assumed top tower attachment (red curves) leads to an inclined response frequency curve in (a) with clear peak and an almost flat and minimized pendulum deflection amplitude in (b). With respect to the lower attachment dof j (magenta curves) the response curve in (a) is almost equally balanced but has clearly too little damping, while its pendulum amplitude curve in (b) has a significant overshoot. The blue curves represent the proposed calibration described next, which seems to provide the optimal compromise between response mitigation and limited pendulum amplitudes.

Consistent modal decomposition

As shown in Fig. 1 the pendulum absorber is attached to the structure at two points (dofs *j* and *k*). In the present approach, the relative absorber motion is defined as the displacement relative to fully restraining the damper deformation, and thus rigidly linking the pendulum mass in Fig. 1 to the tower wall. The transformation that secures the correct relative absorber motion is

$$v = u_a - \mathbf{d}^T \mathbf{u}_s \tag{6}$$

Elimination of the absolute absorber displacement u_a by the relative absorber motion v in (6) gives the modified equations of motion

$$\begin{aligned} \left(\mathbf{M}_s + m_a \mathbf{d}\mathbf{d}^T\right)\ddot{\mathbf{u}}_s + \left(\mathbf{K}_s + k_a \Delta\mathbf{d}\Delta\mathbf{d}^T\right)\mathbf{u}_s + m_a \mathbf{d}\ddot{v} + k_a \Delta\mathbf{d} v &= \mathbf{f}_s \\ m_a \ddot{v} + c_a \dot{v} + k_a v + m_a \mathbf{d}^T \ddot{\mathbf{u}}_s + k_a \Delta\mathbf{d}^T \mathbf{u}_s &= 0 \end{aligned} \tag{7}.$$

where $\Delta\mathbf{dd} = \mathbf{d} - \mathbf{b}$ represents the difference in the connectivity vectors, that vanishes for the classic TMD ($\Delta\mathbf{d} = \mathbf{0}$).

This eigenvalue problem for this alternative representation includes the absorber mass as

$$\left(\mathbf{K}_s - \omega_s^2(\mathbf{M}_s + m_a \mathbf{d}\mathbf{d}^T)\right)\bar{\mathbf{u}}_s = \mathbf{0} \tag{8}$$

with ω_s being the natural frequency for the structure with the augmented mass matrix. An improved representation could be obtained by also including the stiffness term in (7a), which however contains the – to be determined – absorber stiffness k_a. The structural displacement is now expressed by the expansion

$$\mathbf{u}_s = \sum_{j=1}^{N} \frac{\bar{\mathbf{u}}_j}{\nu_j} p_j \qquad , \qquad \nu_j = \mathbf{d}^T \bar{\mathbf{u}}_j \tag{9}$$

with p_j as the modal coordinate, N being the number of terms included and υ_j representing the modal displacement at dof j where the dashpot in Fig. 1 is attached. Substitution of (9) into (7) followed by pre-multiplication with $\bar{\mathbf{u}}_s^T/\nu_s$ gives the following coupled modal equations for the targeted mode shape $j=s$,

$$\begin{aligned} m_s \ddot{p}_s + k_s p_s + k_a \frac{\Delta\nu_s^2}{\nu_s^2} p_s + m_a \ddot{v} + k_a \frac{\Delta\nu_s}{\nu_s} v &= f_s \\ m_a \ddot{v} + c_a \dot{v} + k_a v + m_a \ddot{p}_s + k_a \frac{\Delta\nu_s}{\nu_s} p_s &= 0 \end{aligned} \tag{10}$$

In these modal equations, the change in modal connectivity is defined as $\Delta\nu_s = \Delta\mathbf{d}^T \bar{\mathbf{u}}_s$, while the interaction with other vibration modes is simply neglected in the supplemental (third) stiffness term in (10a) and the (two last) coupling terms in (10b).

The modal truncation creates the difference between the various modelling methods, since as little dynamics as possible should be neglected when truncating the series terms. In the present representation (6) relative to the damper deflection, the truncation is considered robust as it contains the limiting cases with vanishing and infinite absorber damping, whereby the absorber mass is included in the mode shapes by the eigenvalue problem (7). The representation in (6) thus

implies that the damping notoriously only appears in the absorber equation (10b), whereby it must not be omitted in the structural equation (10a).

Absorber calibration

The modal equations in (10) are expressed in the frequency domain with angular frequency ω, whereby variable p_s and v in the following denote the associated steady-state amplitudes. The modal equations can then be expressed as

$$\begin{aligned} \left(-\xi^2+1+\kappa\Delta\gamma^2\right)p_s+\left(-\xi^2\mu+\kappa\Delta\gamma\right)v &= f_s/k_s \\ \left(-\xi^2\mu+i\xi\beta+\kappa\right)v+\left(-\xi^2\mu+\kappa\Delta\gamma\right)p_s &= 0 \end{aligned} \tag{11}$$

in which the non-dimensional frequency is defined as $\xi=\omega/\omega_s$, while the mass, stiffness and damper ratios

$$\mu=\frac{m_a}{m_s} \quad , \quad \kappa=\frac{k_a}{k_s} \quad , \quad \beta=\frac{c_a}{\sqrt{m_s k_s}} \tag{12}$$

Are defined relative to the modal mass and stiffness

$$m_s=\frac{\bar{\mathbf{u}}_s^T(\mathbf{M}_s+m_a\mathbf{d}\mathbf{d}^T)\bar{\mathbf{u}}_s}{\nu_s^2} \quad , \quad k_s=\frac{\bar{\mathbf{u}}_s^T\mathbf{K}_s\bar{\mathbf{u}}_s}{\nu_s^2} \tag{13}$$

The difference in modal deflection is in (11) represented by the relative increment $\Delta\gamma=\Delta\nu_s/\nu_s$. The characteristic equation follows from (11) as

$$\xi^4-\xi^2\frac{\mu+\kappa\left(1+\mu((1-\Delta\gamma)^2-1)\right)}{\mu(1-\mu)}+\frac{\kappa}{\mu(1-\mu)}+i\xi\frac{\beta}{\mu(1-\mu)}\left(-\xi^2+1+\kappa\Delta\gamma^2\right)=0 \tag{14}$$

The desired calibration with equal damping in the two modes associated with the targeted vibration form is in [6, 8, 9] obtained by comparison with the generic quartic polynomial

$$\xi^4-\xi^2\left(2+4\chi^2\right)\xi_0^2+\xi_0^4+i2\sqrt{2}\chi\xi_o\xi\left(-\xi^2+\xi_0^2\right)=0 \tag{15}$$

Comparison of the last parentheses in (14) and (15) defines the reference frequency ratio as $\xi_0^2=1+\kappa\Delta\gamma^2\approx 1$, whereby comparison of the constant terms defines the stiffness ratio

$$\kappa=\mu(1-\mu) \tag{16}$$

which corresponds to the result in [9] for a classic TMD. The attainable damping is subsequently determined by the parameter

$$4\chi^2=\frac{\mu}{1-\mu}\left(1+(1-\mu)\left((1-\Delta\gamma)^2-1\right)\right) \tag{17}$$

For the classic TMD with $\Delta\gamma=0$, the parenthesis in (17) becomes unity, whereby the correction for finite values of $\Delta\gamma$ appears because of the double attachment to dofs j and k in Fig. 1(c). The

Materials Research Proceedings **20** (2022) 39-46 https://doi.org/10.21741/9781644901731-6

explicit solution in (17) is simplified because of the coordinate shift in (6), whereby m_a is contained in the eigenvalue problem (7).

By comparison of the common coefficient to the odd-power terms in the characteristic equations (14) and (15), the damper ratio is finally obtained as

$$\beta = \sqrt{2\mu^3(1-\mu)\Big(1+(1-\mu)\big((1-\Delta\gamma)^2-1\big)\Big)} \tag{18}$$

in which the correction coefficient from (17) is again recognized. This concludes the pendulum absorber tuning, which provides the blue curves in Fig. 2, comprising a suitable compromise between a flat response curve in (a) without any overshoot in (b). It should be noted that the classic TMD stiffness calibration in (5a) gives almost the same mitigation properties, when (5b) is replaced by the corrected damper ratio in (18).

The offshore wind turbine

This section provides the main information about the numerical offshore wind turbine model used to generate the results in Fig. 2. The geometry is shown in Fig. 3 and overall data is provided in Table 1. The top node mass includes the transverse and rotational inertia from the Rotor Nacelle Assembly (M_{RNA} = 450·10^3 kg and J_{RNA} = 120·10^6 kgm^2). The soil foundation is modelled by a Winkler spring layer with distributed stiffness k_s = 200·10^6 (N/m)/m along the bottom h_{soil} = 40m, while water level is at $x = h_{sea}$ = 68m (corresponding to a water depth of 28m).

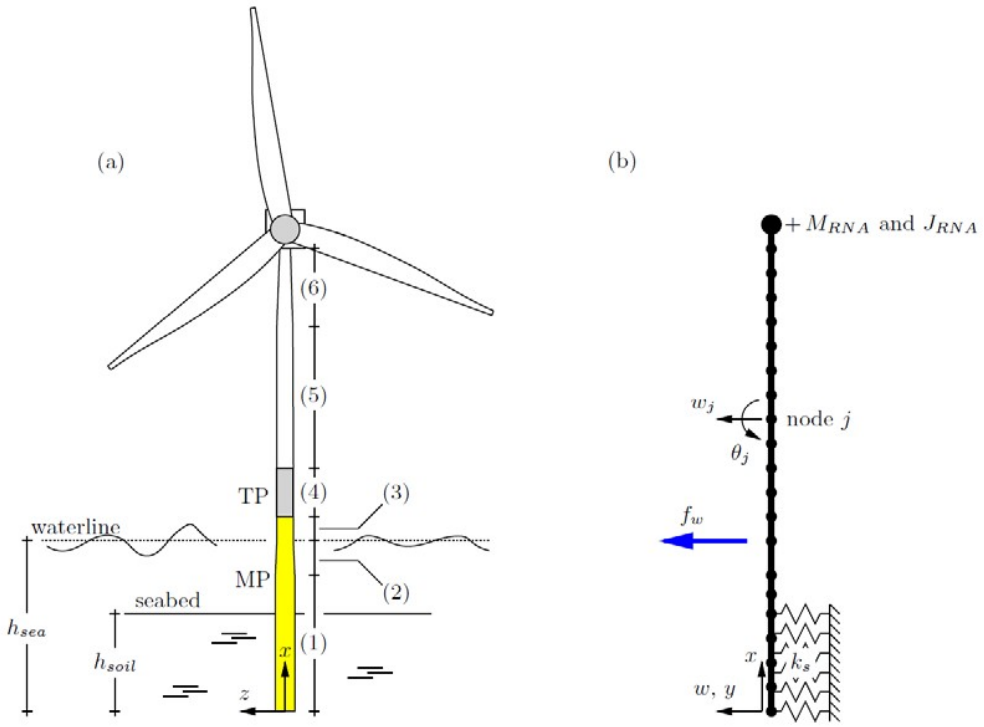

Figure 3: (a) Offshore wind turbine (owt) with data for section (1) to (6) provided in Table 1. The beam element model for the owt is shown in (b), with translation and rotational inerti from the Root Nacelle Assembly (RNA) added to the two top dofs. The model is supported by a Winkler foundation with stiffness k_s.

The owt (monopole + tower) model is discretized by 20 plane beam elements with two nodal dofs (transverse displacement and rotation). The material is steel and as geometric stiffness is neglected, the fundamental natural frequency $\omega_0 = 1.50$ rad/s without the pendulum absorber is slightly larger than in practice. A pendulum mass of $m_a = 10$ ton is assumed, which corresponds to a mass ratio of μ_0=1.54% for the fundamental mode shape with respect to the top transverse displacement. As the length of the pendulum is approximately 22m, it is assumed in this example to simply span the top three beam elements, with attachment dofs in Fig. 1(c) given as $j = 39$ and $k = 45$. In reality, the span length should of course be re-adjusted according to the obtained absorber stiffness k_a. The harmonic load f_w – used to generate the frequency curves of Fig. 2 – is placed locally at sea level $x = h_{sea}$, as shown in Fig. 3(b).

Table 1: Section properties for offshore wind turbine model in Fig. 3.

Section	Height [m]	Outer diameter [mm]	Wall thickness [mm]
		Monopile	
(1) Bottom section	55	8200	75
(2) Conical section	13	8200 → 6500	85
(3) Top section	10	6500	90
(4) Transition piece	19	6500	92
		Tower	
(5) Bottom section	57	6500	55
(6) Conical section	35	6500 → 4200	30

The calibration based on the proposed modal representation gives a mass ratio $\mu = 0.79\%$, thus slightly smaller than $\mu_0 = 0.80\%$ for the TMD calibration based on a TMD mass attachment at the lower dof $j = 39$. The difference occurs because of the addition of the pendulum mass m_a to the mass matrix in (8). The pendulum stiffness $k_a = 22.1$ kN/m is slightly smaller than the value 22.1 kN/m obtained for a TMD placed locally at the top dof $k=45$. This change in stiffness creates the visible inclination of the red curve in Fig. 2(a) and its corresponding overshoot in Fig. 2(b). The actual absorber damping coefficient is found to be $c_a = 2.59$ kNs/m, which is somewhat larger than the simplified TMD solution of 1.87 kNs/m, associated with the placement at dof $j = 39$. The present calibration method therefore consistently incorporates that the pendulum absorber acts on the tower at two different positions, whereby it basically determines an absorber stiffness associated with the top deflection and a damper value that is proportional to the deflection at damper position. It should be emphasized that the classic TMD tuning procedure is incapable of accounting for this effect as it notoriously assumes a single point of attachment of the classic TMD.

Summary

A consistent absorber calibration procedure is devised for an absorber with two different points of attachment. The calibration procedure is illustrated for a simple offshore wind turbine model with a pendulum-type absorber attached to the top tower position and with the dashpot acting horizontally between tower wall and pendulum mass. The proposed calibration formulae are seen to provide a good compromise between effective response mitigation and limited pendulum vibration amplitudes. The concept can be generalized to flexible absorbers with no common or even with distributed points of attachment to the host structure.

References

[1] S. Elias, V. Matsagar, Research developments in vibration control of structures using passive tuned mass dampers, Annual Reviews in Control 44 (2017) 129-156. https://doi.org/10.1016/j.arcontrol.2017.09.015

[2] S. Park, M.A. Lackner, P. Pourazarm, A.R. Tsouroukdissian, J. Cross-Whiter, An investigation on the impacts of passive and semiactive structural control on a fixed bottom and a floating offshore wind turbine, Wind Energy (2019). https://doi.org/10.1002/we.2381

[3] L.K. Wang, W.X. Shi, X.W. Li, Q.W. Zhang, Y. Zhou, An adaptive-passive retuning device for a pendulum tuned mass damper considering mass uncertainty and optimum frequency, Structural Control and Health Monitoring 26 (2019) e2377. https://doi.org/10.1002/stc.2377

[4] S. Colwell, B. Basu, Tuned liquid column dampers in offshore wind turbines for structural control, Engineering Structures 31 (2009) 358-368. https://doi.org/10.1016/j.engstruct.2008.09.001

[5] J.P. Den Hartog, Mechanical Vibrations, fourth ed., Dover, New York, 1985.

[6] S. Krenk, Frequency analysis of the tuned mass damper, Journal of Applied Mechanics 72 (2005) 936-942. https://doi.org/10.1115/1.2062867

[7] M. Zilletti, S.J. Elliott, E. Rustighi, Optimisation of dynamic vibration absorbers to minimise kinetic energy and maximise internal power dissipation, Journal of Sound and Vibration 331 (2012) 4093-4100. https://doi.org/10.1016/j.jsv.2012.04.023

[8] S. Krenk, J. Høgsberg, Tuned resonant mass or inerter-based absorbers: unified calibration with quasi-dynamic flexibility and inertia correction, Proceedings of the Royal Society A - Mathematical, Physical and Engineering Sciences 472 (2016) paper no. 20150718 (23pp). https://doi.org/10.1098/rspa.2015.0718

[9] D. Hoffmeyer, J. Høgsberg, Calibration and balancing of multiple tuned mass absorbers for damping of coupled bending-torsion beam vibrations, submitted for publication (2019). https://doi.org/10.1115/1.4046752